Field Testing of Nano-PCM-Enhanced Building Envelope Components in a Warm-Humid Climate

Kaushik Biswas, PhD
Associate Member ASHRAE

Jue Lu, PhD

Parviz Soroushian, PhD

ABSTRACT

The U.S. Department of Energy Building Technologies Program's goal of developing high-performance, energy-efficient buildings will require more cost-effective, durable, energy-efficient building envelopes. Forty-eight percent of the residential end-use energy consumption is spent on space heating and air conditioning. Reducing envelope-generated heating and cooling loads through application of phase-change material (PCM) enhanced envelope components can facilitate maximizing the energy efficiency of buildings. Field testing of prototype envelope components is an important step in estimating their energy benefits.

An innovative PCM (nano-PCM) was developed with PCM encapsulated with expanded graphite (interconnected) nanosheets, which is highly conducive for enhanced thermal storage and energy distribution, and is shape-stable for convenient incorporation into lightweight building components. During 2012, two test walls with cellulose cavity insulation and prototype PCM-enhanced interior wallboards were installed in a natural exposure test (NET) facility in Charleston, SC. The first test wall was divided into four sections separated by wood studs and thin layers of foam insulation. Two sections contained nano-PCM-enhanced wallboards: one was a three-layer structure in which nano-PCM was sandwiched between two gypsum boards, and the other one had PCM dispersed homogeneously throughout graphite nanosheet-enhanced gypsum board. The second test wall also contained two sections with interior PCM wallboards; one contained nano-PCM dispersed homogeneously in gypsum and the other was gypsum board containing a commercial microencapsulated PCM (MEPCM) for comparison. Each test wall contained a section covered with gypsum board on the interior side that served as control or a baseline for evaluation of the PCM wallboards. The walls were instrumented with arrays of thermocouples and heat flux transducers. This paper presents the measured performance and analysis to evaluate the energy-saving potential of the nano-PCM-enhanced building components.

INTRODUCTION

According to the 2009 Residential Energy Consumption Survey (RECS) of the U.S. Energy Information Administration (EIA), about 48% of the total residential site energy consumption is due to space heating and air conditioning (EIA 2009). The U.S. Department of Energy (DOE) Building Technologies Program's goal of developing high-performance, energy-efficient buildings will require more cost-effective, durable, energy-efficient building envelopes. Application of phase-change materials (PCMs) to building envelopes to take advantage of their high latent heat capacities in reducing the envelope-generated heating and cooling loads has received a lot of attention in the last two decades (Zhou et al. 2007).

Sharma et al. (2009) and Xin et al. (2009) reviewed the research and analysis of available thermal storage systems incorporating PCMs for building applications. Different approaches to PCM applications in building envelopes have been investigated: PCM wallboards (Stovall and Tomlinson 1995; Zhou et al. 2007), PCM mixed with loose-fill insulation (Shrestha et al. 2011), macro-packaged PCM in plastic pouches (Kosny et al. 2012), etc.

The subject of this article is an innovative PCM (nano-PCM) with the PCM encapsulated in expanded graphite

Kaushik Biswas *is a research and development associate (building scientist) at Oak Ridge National Laboratory, Oak Ridge, TN.* ***Jue Lu*** *is a senior scientist at and* ***Parviz Soroushian*** *is the president of Technova Corporation, Lansing, MI.*

Published by ASHRAE 2013

nanosheets, which is highly conductive, for enhanced thermal storage and energy distribution and is shape-stable for convenient incorporation into lightweight building components. This nano-PCM was incorporated in gypsum boards, which are commonly used as interior wallboards on walls in residential construction. Three prototype nano-PCM-enhanced interior wallboards were produced and were installed in a natural exposure test (NET) facility in Charleston, SC, for testing. For comparison, two types of control panels were installed: gypsum board incorporating a commercial microencapsulated PCM (MEPCM) (Micronal® PCM [BASF 2013]) and standard gypsum board. In the subsequent analysis and discussion, these PCM wallboards will be referred to using the following list:

- PCM-Soaked Gypsum
- Three-Layer Structure
- Dispersed Nano-PCM
- MEPCM in Gypsum

The first two products were installed in January 2012 and the latter products were installed in July 2012. The fourth product was also used as a control. Brief descriptions of the PCM products are provided in the following section.

DESCRIPTIONS OF THE PCM PROTOTYPE SAMPLES

Following are brief descriptions of and details about the material and thermophysical characteristics of the PCM wallboards.

Materials

Gypsum powder was used for fabrication of gypsum board. A paraffin, n-heptadecane ($C_{17}H_{36}$), was used as the PCM. High thermal conductivity is a desirable characteristic of PCMs in energy storage applications, but the lower conductivity of paraffins decreases the rates of heat stored and released during the phase-change processes and limits their utility areas (Zalba et al. 2003; Sari and Karaipekli 2007). Exfoliated graphite nanoplatelets (xGnP) (Kim and Drzal 2009) and expanded graphite (interconnected) nanosheets (Drzal and Fukushima 2009) were added for increasing the thermal conductivity of the PCM wallboards for enhanced heat transfer and better utilization of PCMs.

PCM-Soaked Gypsum

This PCM wallboard is comprised of gypsum board that absorbed 20%-by-weight n-heptadecane by soaking. The board composition was 99% gypsum and 1% xGnP for enhanced thermal conductivity. The xGnP was dispersed in 1 g/L sulfonated polystyrene by tip sonication (using ultrasound energy for particle dispersion) for one hour and then mixed with the gypsum powder and water. The board was cured overnight at room temperature, followed by curing at 50°C for 48 hours. After cooling down to room temperature, the board was soaked in melted n-heptadecane, with a final PCM content of 20% by weight. Figure 1 shows the heat flow data from differential scanning calorimetry (DSC) testing of n-heptadecane. During melting, the n-heptadecane is trapped in the air voids of the gypsum matrix without weeping due to capillary action and surface tension.

Three-Layer Structure

This wallboard contained a 4 mm layer of nano-PCM sandwiched between two 5 mm layers of gypsum. The nano-PCM contains 8%-by-weight expanded graphite nanosheets and 92%-by-weight n-heptadecane. Expanded graphite nanosheets were processed following a microwave process from expandable graphite (Drzal and Fukushima 2009). The weight percentage of nano-PCM in the wallboard was about 20%. Figure 1 shows the heat flow data from DSC testing of the nano-PCM. The positive heat flows represent exothermic conditions, indicating the freezing phenomenon of the nano-PCM; negative heat flows indicate a melting process. The

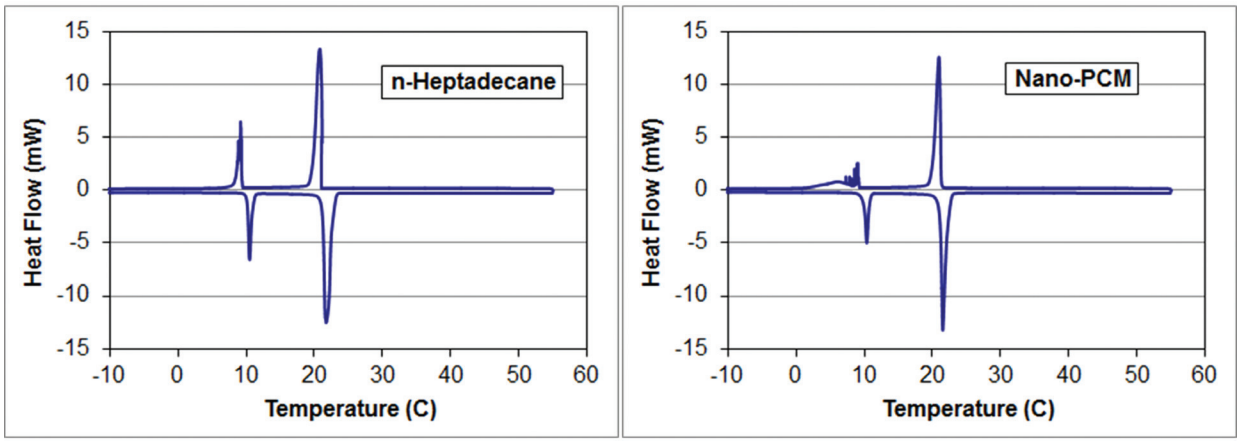

Figure 1 *Melting and freezing characteristics (DSC curve) of n-heptadecane (left) and nano-PCM (n-heptadecane with 8%-by-weight expanded graphite nanosheets) (right). The DSC heating and cooling rate was 1°C/min.*

DSC data provide information about the active temperature range of the PCM (where phase changes occur) and the respective latent heats. For design and analysis purposes, the smaller peaks on the left of the major melting and freezing peaks have been ignored.

Dispersed Nano-PCM

This board contains 20%-by-weight nano-PCM homogeneously dispersed in gypsum board. Gypsum powder was mixed with 65%-by-weight water, followed by an addition of nano-PCM. This board was cured for one week at room temperature. The DSC data for this product are shown in Figure 2.

MEPCM in Gypsum

This is gypsum board incorporating 20%-by-weight MEPCM (Micronal®). This board was intended for use as another control, in addition to regular gypsum board, to evaluate the performance of three prototype PCM wallboards (PCM-soaked gypsum, three-layer structure, and dispersed nano-PCM). This board was cured overnight at room temperature then for five hours at 50°C. Figure 2 shows the DSC data for the MEPCM in gypsum product.

Table 1 lists the thermophysical properties of the PCM wallboards. The properties were estimated using DSC data at 1°C/min heating and cooling rates. The melting and freezing onset temperatures were determined using an integration function based on a tangents method that is included in the DSC analysis software.

TEST FACILITY AND TEST WALL DETAILS

These wall tests are ongoing in a NET facility in Charleston, SC, shown in Figure 3. NET facilities expose side-by-side roof/attic and wall assemblies to natural weathering in four different humid U.S. climates. The data from these facilities help the industry develop products to avoid adverse moisture-related impacts in buildings and are essential in validating hygrothermal and energy models. NET structures are located at Oak Ridge, TN; Charleston, SC; Tacoma, WA; and Syracuse, NY. Each is temperature and humidity controlled and instrumented to measure moisture content in materials, vapor pressure, temperature, heat flux, humidity, etc. Figure 3 shows the south wall of the Charleston NET facility, representing a warm-humid climate, which houses multiple side-by-side test walls. Also shown is a weather station on the west gable end of the building.

The test walls were built using wood framing (2 × 6 studs) with oriented strand board (OSB) on the outside and PCM wallboards on the inside. The outer side of the OSB is covered with a weather-resistant barrier and vinyl siding. Figure 4 shows the installed test walls. On the left is the first wall, marked as *test wall 1*, which was built in January 2012. It was divided into four equal sections; two sections were covered with the PCM-soaked gypsum and three-layer structure PCM wallboards, and another section was covered with standard gypsum board. The second wall, *test wall 2*, was installed

Table 1. PCM Properties

	Latent Heat, J/g		Phase-Change Onset, °C	
	Melting	**Freezing**	**Melting**	**Freezing**
PCM- Soaked Gypsum	28.2	27.9	21.2	21.2
Three-Layer Structure	29.2	29.3	21.1	21.3
Dispersed Nano-PCM	26.9	26.8	21.1	21.3
MEPCM in Gypsum	18.8	18.9	18.9	20.9

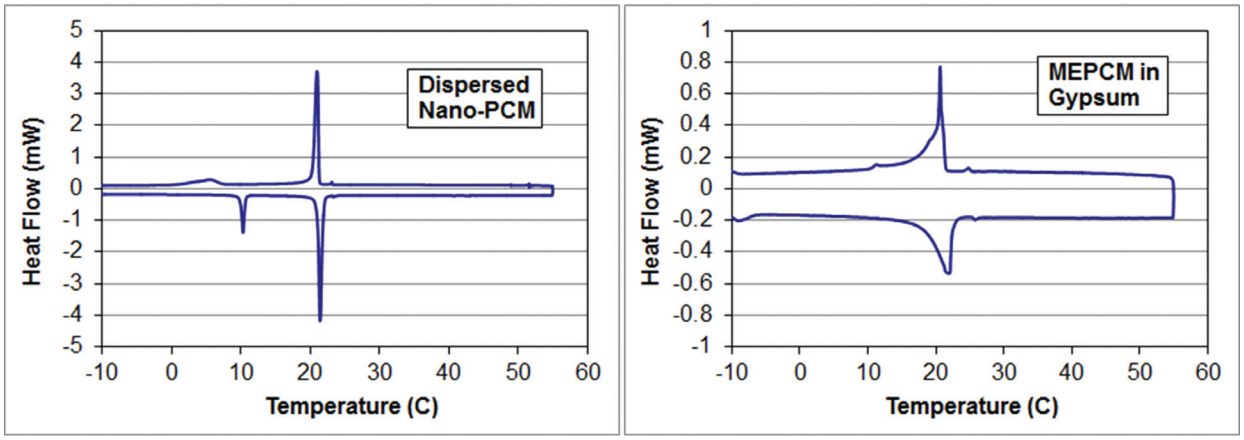

Figure 2 *Melting and freezing characteristics (DSC curves) of the dispersed nano-PCM wallboard (left) and MEPCM in gypsum wallboard (right). The DSC heating and cooling rate was 1°C/min.*

during July 2012 and contained the dispersed nano-PCM and MEPCM in gypsum wallboards, along with a taller gypsum section.

The smaller wall cavities are about 1.1 m high and 0.4 m wide, and the taller gypsum-covered cavity in test wall 2 is 2.2 m high and 0.4 m wide. Each cavity or section is separated from the others using wood studs and thin layers of foam insulation. The cavity depth is 14 cm. During construction, each wall cavity was covered with a plastic mesh and then cellulose insulation was added by cutting a slot in the mesh at the top of the cavity. The cellulose was allowed to settle under its own weight. The measured cavity volume and estimated weight of cellulose insulation added to the cavities yielded an average density of 40.9 kg/m^3. It should be noted that, due to the ad-hoc application method, the resulting density was lower than the recommended density for blown-in dense-packed cellulose, which is about 56.1 kg/m^3. The area surrounding the test cavities was filled with fiberglass insulation to prevent convection loops in empty air spaces and minimize the thermal interaction with the neighboring test wall sections. The perimeter cavities are used for routing instrumentation cables, and fiberglass batts were used to fill those perimeter cavities due to ease of installation.

Figure 3 *Charleston, SC, NET facility.*

DATA ACQUISITION SYSTEM AND INSTRUMENTATION

Figure 5 shows a typical instrumentation layout in the wall cavities. The wall has vinyl siding and a weather barrier over OSB on the exterior side of the wall, which is exposed to the atmosphere (as seen on the south wall in Figure 3). The interior side is covered with a gypsum board. Each cavity contains a thermistor and relative humidity sensor combination (T/RH sensor) on the OSB and gypsum surfaces facing the cavity, a thermistor inside the cavity (mid-depth) and on the gypsum surface facing the room interior, and heat flux transducers (HFTs) on the gypsum surface facing the cavity. Within each cavity, these sensors are located approximately in a line along both the vertical and horizontal midpoints of the cavity. In addition, a single thermistor is attached to the wall exterior (between the OSB and exterior siding) and a T/RH sensor combination is attached on the OSB surface facing the exterior (not shown in Figure 5). The T/RH sensors are indicated by the white packets seen in Figure 5.

In addition to the sensors attached to the test wall, the NET facility is equipped with sensors and instruments to monitor the local weather conditions, including temperature, humidity, solar irradiance, wind conditions, etc. These sensors are controlled and monitored by dataloggers and multiplexers. Each sensor is scanned at five-minute intervals, and the data are averaged and stored at hourly intervals. The data are downloaded on a weekly basis at Oak Ridge National Laboratory

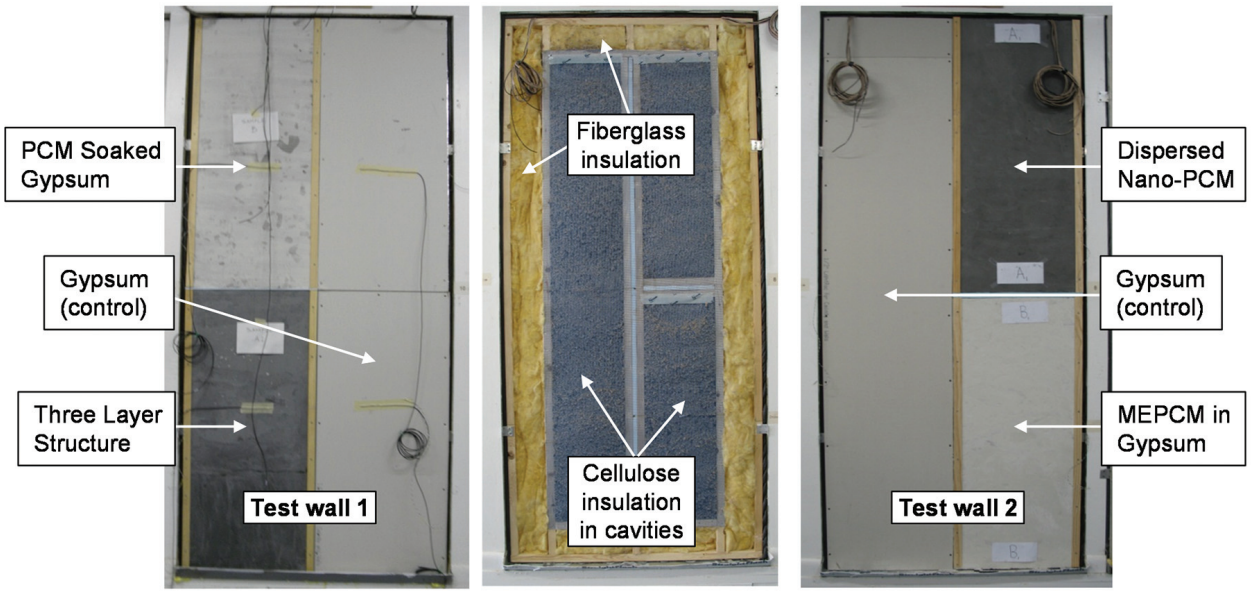

Figure 4 *Test walls with the different PCM prototype wallboards.*

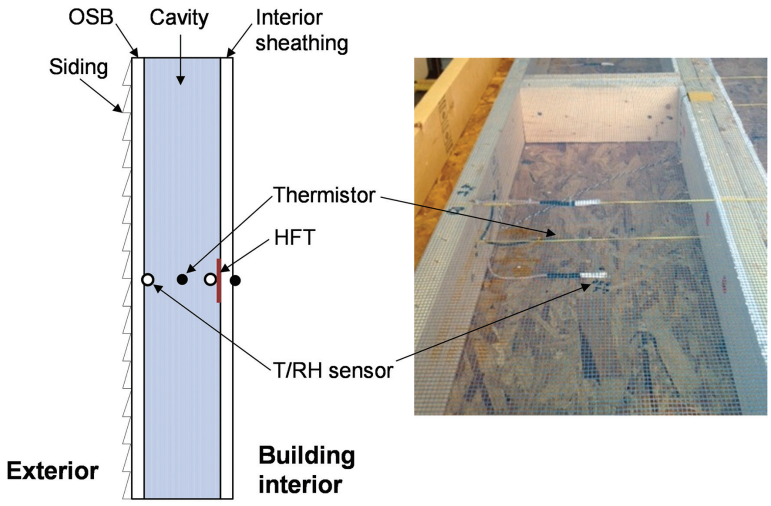

Figure 5 *Sensor placement in test wall cavities.*

(ORNL) using a dedicated computer and modem. Table 2 provides the sensor specifications. The HFTs were calibrated using a heat flowmeter apparatus (HFMA) sandwiched by insulation and regular gypsum board. The HFMA is used for thermal transmission property measurements following the ASTM C518 (2010) test method and is accurate within 1%. The HFMA consists of two independently temperature-controlled plates, both of which are equipped with heat flow sensors. The calibration constants of the HFTs used in the Charleston test walls were obtained by correlating the measured heat flows of the HFMA to the HFT voltage outputs.

RESULTS AND DISCUSSION

This section describes the temperature and heat flux data from the test walls to examine the behavior and impact of the PCM prototype wallboards. The data are compiled into weekly files containing hourly-averaged data. The period covered in this section is July–December 2012, after the installation of the second test wall. This period is deemed sufficient for the weather-related evaluation of the PCM products as it includes summer, winter, and shoulder (fall) months. The focus is on summer and winter periods, when the cooling and heating loads are at their peak.

Temperature Distribution and PCM Behavior

The temperature distributions in the different sections of the two test walls are shown in Figures 6 and 7. The hourly-averaged temperature data are shown for a typical summer week (July 18–25). The temperatures are shown at the wall exterior, the OSB interior (facing the cavity), the cavity center, the wallboard exterior (facing the cavity), and the wallboard interior (facing the room).

The room interior was maintained at about 20°C–22°C during the monitoring period. A clear trend is seen in the temperatures from the exterior to the interior. Some differences are seen in the cavity center and the wallboard exterior between the different test walls and the test sections. However, these differences are fairly insignificant and do not reveal much about the behavior and impact of the PCMs in the different wallboards.

Table 2. Installed Sensor Accuracy

	Accuracy	Sensitivity	Repeatability
10 K ohm Thermistor	± 0.2%	—	± 0.2%
Humidity Sensor	± 3.5%	—	± 0.5%
Heat Flux Transducer	± 5%	5.7 (W/m^2)/ mV	—
Outdoor Relative Humidity Sensor	± 3%	—	—
Solar Pyranometer, Vertical	± 3%	0.2 (kW/m^2)/ mV	—
Solar Pyranometer, Horizontal	± 3%	10 μV/(W-m^2)	—
Channel Multiplexer	± 0.1% of Full Scale Reading	—	—

To further examine the PCM behavior, the wallboard exterior and interior temperatures are shown in Figure 8, along with the corresponding melting and freezing onset temperatures. The data shown in Figure 8 were compiled from the weekly data files from July 11 to December 26, 2012.

For maximum benefit from a PCM, it needs to melt and freeze on a diurnal basis, i.e., its temperature should rise above its melting point and fall below its freezing point on a daily basis. The hourly variations of the exterior and interior surface

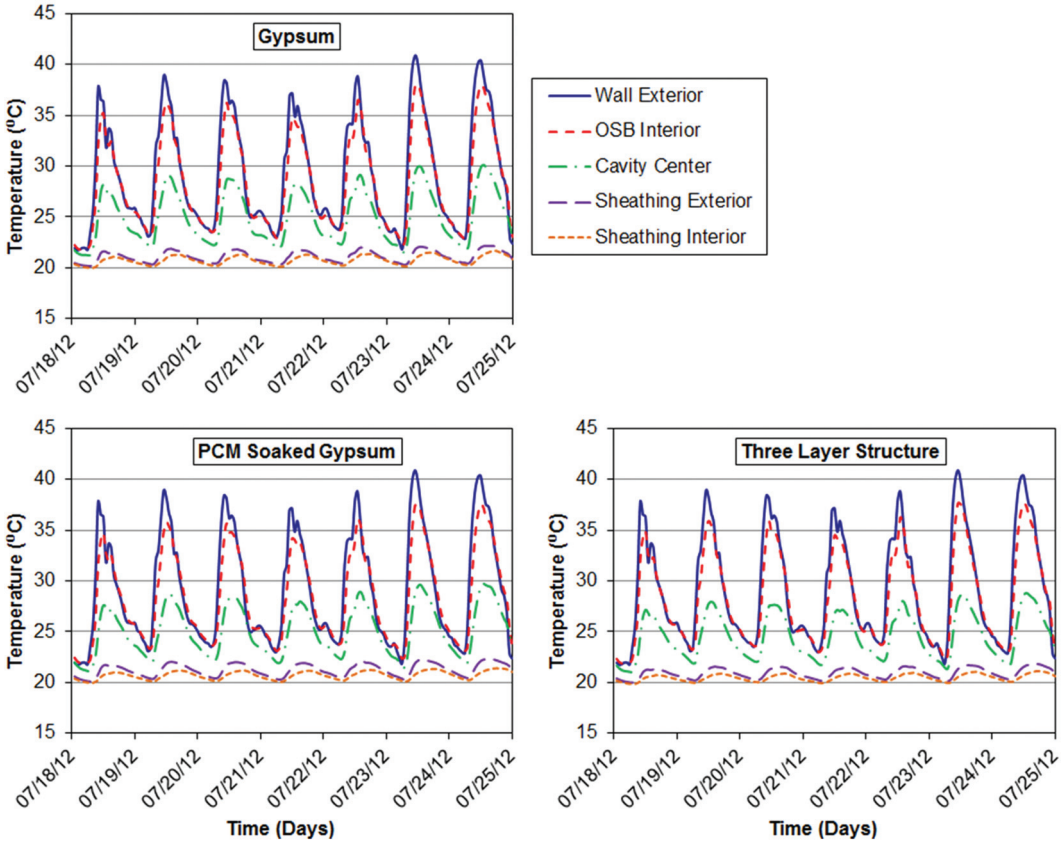

Figure 6 *Temperature distribution in different sections of test wall 1.*

temperatures compared to the phase-change onset temperatures can provide information about the effectiveness of the PCM prototype wallboards. The first plot in Figure 8 shows the behavior of the PCM-soaked gypsum wallboard. The exterior temperatures cycled above the melting onset temperature and below the freezing onset temperature almost every day during the summer months (July–September) and periodically in October, indicating frequent phase-change activity near the surface of the wallboard facing the cavity. The interior wallboard temperatures, however, remained predominantly below the melting onset temperature during this time. From November onwards, the wallboard temperatures stayed predominantly below the melting onset temperature, and the PCM can be expected to have been frozen during this time.

The second plot shows the behavior of the three-layer structure wallboard. The interior wallboard temperature remained below the melting point at all times. The exterior wallboard temperature cycled above and below the phase-change temperatures from July till early October but remained below the melting point after that. The dispersed nano-PCM wallboard had melting and freezing onset temperatures similar to those of the three-layer structure wallboard. The diurnal exterior and interior temperature oscillations were greater such that the exterior temperatures rose above and below the melting and freezing onset temperatures from July through early November. Even the interior temperatures rose above the melting point several times July through September.

The fourth plot shows the temperatures of the MEPCM in gypsum wallboard. This product has the lowest melting onset temperatures of all the wallboards, with the result that both exterior and interior wallboard temperatures were predominantly above the melting point. The wallboard temperatures cycled above and below the freezing onset temperature on a daily basis from July till early October and less frequently from October to mid-November, then remained below the freezing point after that. Thus, unlike the other PCM products, the MEPCM in gypsum wallboard can be expected to have undergone at least partial melting and freezing even during the winter period.

In summary, the temperature data indicate that the first three wallboards underwent at least partial melting and freezing between July and mid-November, especially near the exterior surface facing the wall cavities, and remained predominantly frozen thereafter. The MEPCM in gypsum wallboard, however, showed phase-change activity throughout the evaluation period.

Heat Flux Variation

In this section, data from the HFTs installed in the test cavities are shown and described. It should be noted that the

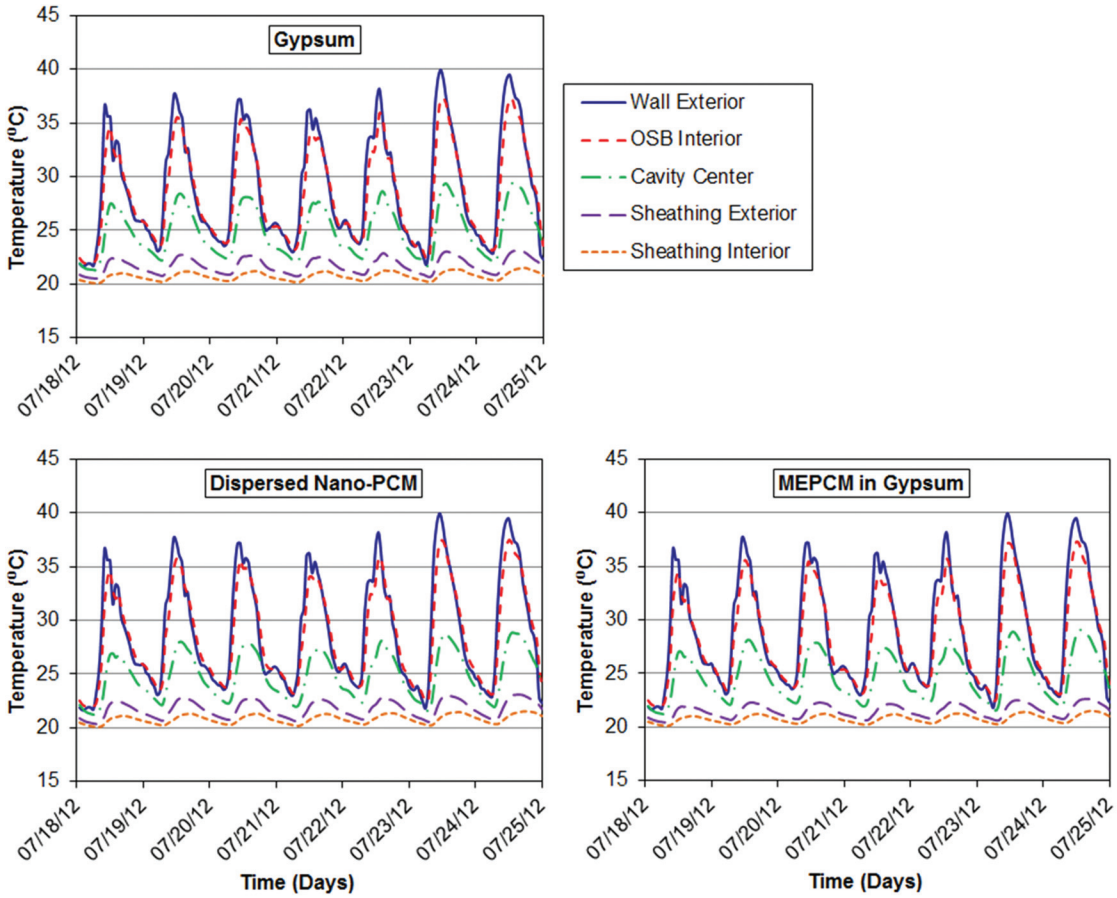

Figure 7 *Temperature distribution in different sections of test wall 2.*

HFTs measuring the heat flux were installed on the exterior surface of the wallboards (facing the cavity). From a space-conditioning perspective, the heat flux that actually enters the conditioned area is of primary interest. In the test sections, since the PCMs are contained in the wallboards, the locations of the HFTs are not ideal, as they do not fully capture the impact of the melting and freezing of PCMs on the heating and cooling loads in the conditioned area. The HFTs only capture the heat flow between the wallboard and the cavity, which may be different from the heat flow at the wallboard interior due to the latent heat storage/release within the wallboards.

Figures 9 and 10 show the hourly heat fluxes during a summer and winter week, respectively, through the different test sections in the two test walls, test wall 1 and test wall 2. The control gypsum test sections are shown for comparison. Also shown is the hourly solar irradiance on the test wall exteriors. As expected, the daytime heat fluxes show a strong correlation with the solar irradiance.

In Figure 9, the first plot shows the test sections in test wall 1. The behavior of the three-layer structure wallboard is similar to the control gypsum section, but the peak daytime heat gains in the PCM-soaked gypsum section are higher by up to 30% compared to the control. Both PCM wallboards in test wall 2 reduced the peak daytime heat gains by about 20% compared to the gypsum section, which is beneficial in reducing the cooling loads on the conditioned space.

Figure 10 shows the heat flux variations during a winter week. There was very little heat gain measured by the HFTs during this week, with substantial heat losses, especially during the night. The daytime peaks were similar between the PCM wallboards and their respective control sections. In test wall 1, both PCM wallboard sections exhibited greater peak heat losses compared to the gypsum control; conversely, in test wall 2, both PCM sections reduced the heat losses at night compared to the gypsum section.

To further investigate the impact of the PCM-enhanced wallboards, the heat flux data though the different wall sections were integrated over 30-day winter and summer periods to determine the total heat gains and losses through the different sections. The integration was performed using the trapezoidal rule:

$$\text{Total Integrated Heat Flow, } Q \text{ [kJ/m}^2\text{]} = \sum_{n=0}^{m} 0.5 \times \Delta X_n \times (Y_n + Y_{n+1}) \quad (1)$$

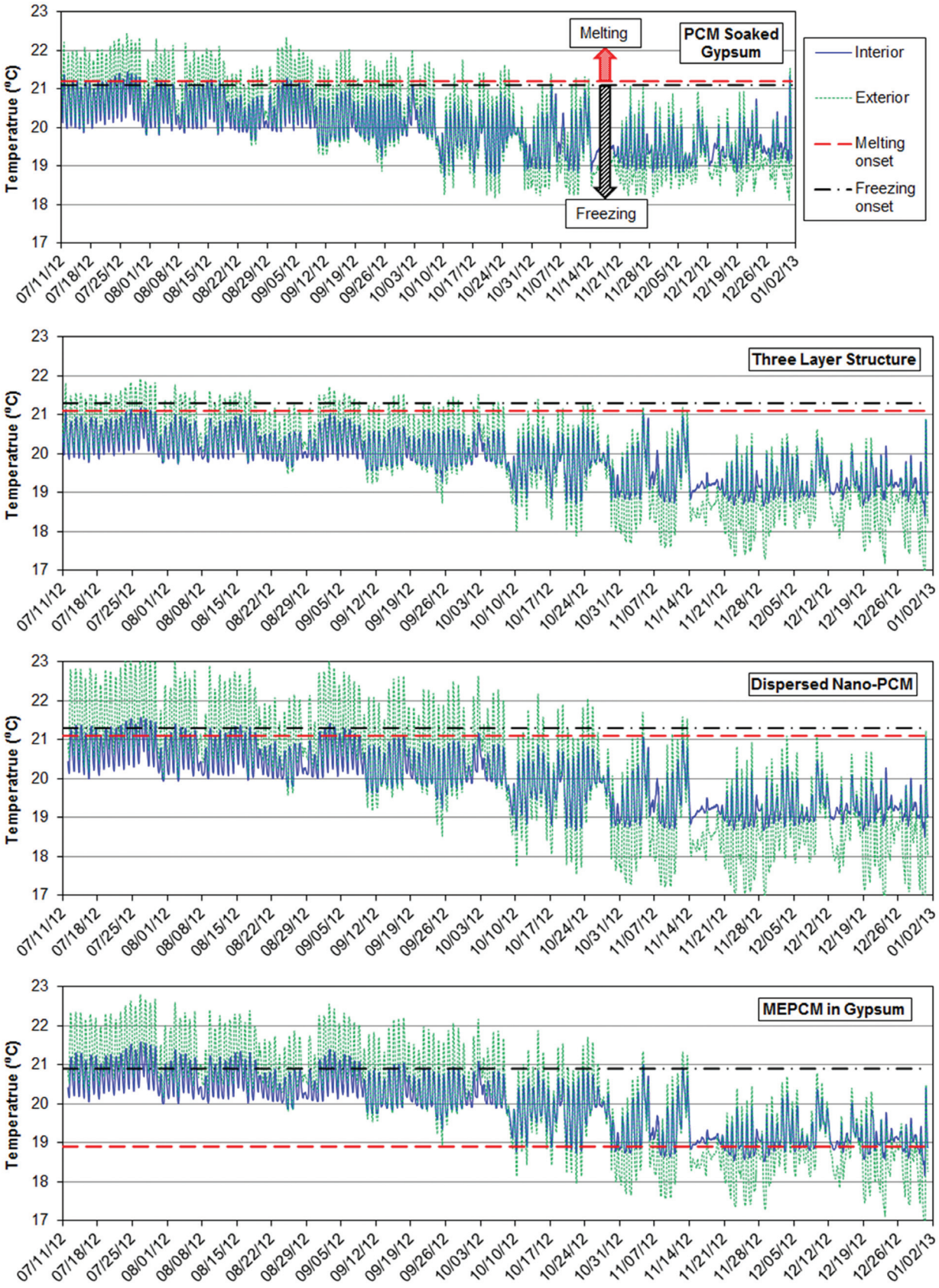

Figure 8 *Comparison of PCM-enhanced wallboard interior and exterior temperatures with their respective phase-change onset temperatures.*

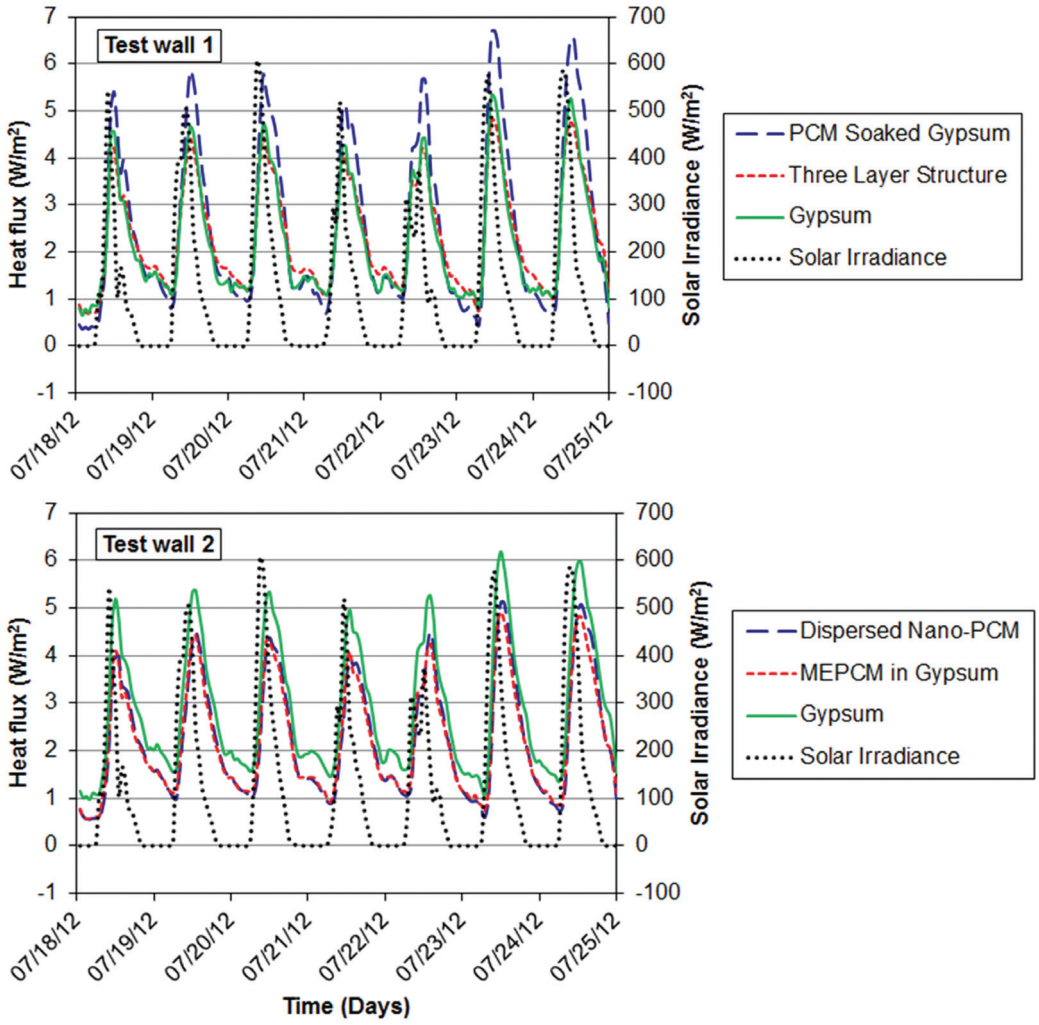

Figure 9 *Summer heat flux variation and solar irradiance.*

In Equation 1, Y_n and Y_{n+1} correspond to the heat flux during current and future time steps, ΔX_n is the time step (1 h in this case), and the subscript m denotes the final point in the series, which varies depending on the summer or winter data sets. The positive and negative heat fluxes were integrated separately to determine the heat gains and losses for each section. The integrated or total heat gains and losses and the net heat transfer during summer and winter periods are shown in Tables 3 and 4. The net heat transfer for each period was obtained by integrating the positive and negative heat fluxes together. Also shown in the tables are the percent reductions compared to the respective gypsum control sections.

Using the general uncertainty analysis method described by Coleman and Steele (1989), the uncertainty (U_Q) in the integrated heat flow (Q) can be described by:

$$U_Q^2 = \left[\left(\frac{\partial Q}{\partial Y_n} U_Y\right)^2 + \left(\frac{\partial Q}{\partial Y_{n+1}} U_Y\right)^2\right]^{1/2} \qquad (2)$$

Assuming a 5% uncertainty (U_Y) in the HFT measurements, the uncertainty of the integrated heat flows reported in Tables 3 and 4 is 7.1%.

Thirty-day periods were chosen that represent typical summer and winter conditions to analyze the data. The 30-day summer period extended from July 13 to August 11, 2012, and the winter period was December 2–31, 2012. Table 3 lists the integrated heat flows from test wall 1. Clearly, neither PCM wallboard performed as well as expected, allowing both higher heat gains during summer and higher heat losses during winter. Both PCM wallboards used in test wall 2 performed better than the gypsum control (Table 4), with about 21%–26% reductions in heat gain and heat loss during the cooling and heating seasons, respectively. The prototype dispersed nano-PCM wallboard performed better than the wallboard with the commercially available MEPCM in reducing both heating and cooling loads.

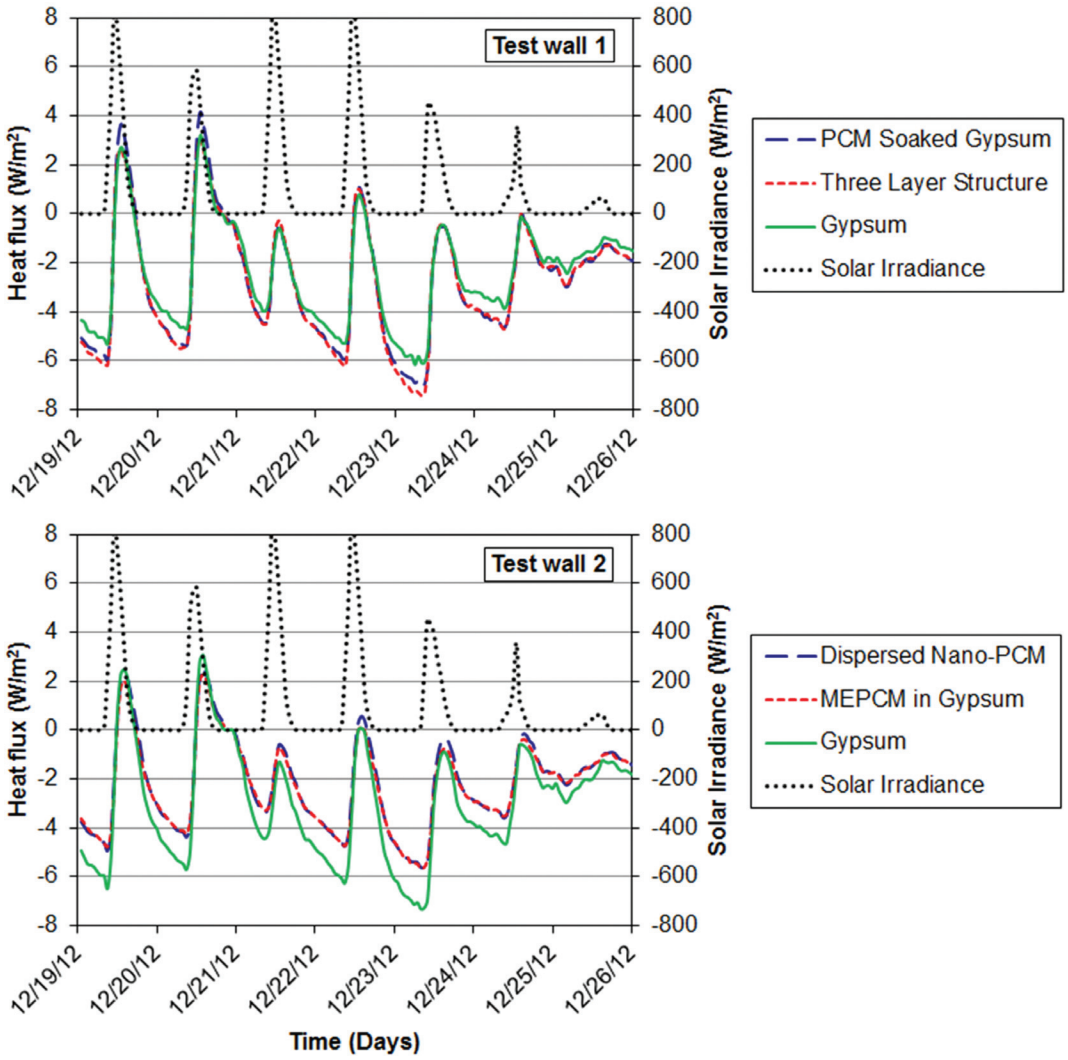

Figure 10 *Winter heat flux variation and solar irradiance.*

Table 3. Heat Flux Statistics for Test Wall 1

	Heat Gain, kJ/m²	% Reduction	Heat Loss, kJ/m²	% Reduction	Net, kJ/m²	% Reduction
Summer 30-Day Period (July 13–August 11, 2012)						
PCM-Soaked Gypsum	5839.6	–9.76	–6.6		5832.9	–9.63
Three-Layer Structure	5459.5	–2.61	–0.7		5458.8	–2.60
Gypsum	5320.4		0.0		5320.4	
Winter 30-Day Period (December 2–31, 2012)						
PCM-Soaked Gypsum	633.2	–36.59	–5727.3	–17.12	–5094.1	–15.08
Three-Layer Structure	483.9	–4.38	–5780.5	–18.21	–5296.6	–19.66
Gypsum	463.5		–4890.1		–4426.5	

Table 4. Heat Flux Statistics for Test Wall 2

	Heat Gain, kJ/m^2	% Reduction	Heat Loss, kJ/m^2	% Reduction	Net, kJ/m^2	% Reduction
Summer 30-Day Period (July 13–August 11, 2012)						
Dispersed Nano-PCM	5263.0	22.86	–0.2		5262.8	22.86
MEPCM in Gypsum	5336.2	21.78	0.0		5336.2	21.78
Gypsum	6822.3		0.0		6822.3	
Winter 30-Day Period (December 2–31, 2012)						
Dispersed Nano-PCM	453.9	5.65	–4333.0	25.88	–3879.1	27.70
MEPCM in Gypsum	406.9	15.42	–4403.5	24.68	–3996.6	25.50
Gypsum	481.0		–5846.0		–5365.0	

It is again noted that the heat fluxes shown in Figures 9 and 10 and the integrated heat flows listed in Tables 3 and 4 are not truly representative of the heat addition to or loss from the conditioned space, due to the location of the HFTs. Further, the positive daytime heat flows measured in the PCM sections during summer may be augmented if the PCM was melting and absorbing heat at the cavity-wallboard interface. Conversely, the nighttime losses may include the heat released at the cavity-wallboard interface due to the freezing of the PCM.

FUTURE WORK

In its current form, this paper describes a work-in-progress project. Further analyses and measurements will enable a better understanding of the behavior of the PCM prototypes being studied. The next step in the process is developing a numerical model of the test walls, with appropriate thermophysical properties of the PCM prototypes, followed by validation studies using the field test data. The numerical model can provide information about the actual impact of the PCM products on the annual heating and cooling loads in the test building. Measurements of the thermal conductivity (in the fully frozen and fully melted states) and temperature-dependent specific heat of the PCM products will enable better understanding of the field data and are essential for accurate modeling of the test walls.

CONCLUSIONS

This paper describes the testing of four prototype PCM-enhanced interior wallboards in a natural exposure test facility in Charleston, SC. Two test walls were built using wood-frames with cellulose cavity insulation. The walls were divided into sections, each containing one of the PCM wallboards. The PCM wallboards were produced by combining gypsum boards with PCMs using different techniques. Based on the PCM incorporation method, the wallboards were referred to as PCM-soaked gypsum, three-layer structure, dispersed nano-PCM, and MEPCM in gypsum. Each test wall also contained a section covered with regular gypsum board that served as control to evaluate the test sections with the PCM wallboards. The walls were instrumented using temperature and heat flux sensors. The temperature data revealed that all four PCM wallboards were expected to have undergone at least partial phase-change phenomenon during the summer and shoulder months; the MEPCM in gypsum wallboard exhibited phase-change activity even during winter, unlike the PCM in the other wallboards, which remained frozen. The heat flux data indicated that the dispersed nano-PCM reduced the space-conditioning loads compared to a standard gypsum board and also performed better than the control wallboard incorporating a commercial microencapsulated PCM. However, the PCM-soaked gypsum and three-layer structure did not perform very well compared to the corresponding gypsum control section. Numerical modeling and validation studies using the test data can provide valuable information about the actual impact of the PCM wallboards on the building heating and cooling loads.

ACKNOWLEDGMENTS

The authors would like to acknowledge the funding support for this work from the Department of Energy Small Business Innovation and Strategies Program (Recovery Act) Award No. DE-SC0003309. The contributions of Jerald Atchley and Phillip Childs of ORNL in installing and instrumenting the test walls, data gathering, and troubleshooting are also gratefully acknowledged.

REFERENCES

ASTM. 2010. ASTM C518-10, *Standard Test Method for Steady-State Thermal Properties by Means of the Heat Flow Meter Apparatus*. West Conshohocken, PA: ASTM International.

Coleman, H.W. and W.G. Steele, 1989. Experimentation and Uncertainty Analysis for Engineers. John Wiley & Sons, New York.

Drzal, L., and H. Fukushima. 2009. Expanded graphite and products produced therefrom. US Patent 7,550,529 B2.

Kim, S., and L. Drzal. 2009. High latent heat storage and high thermal conductive phase change materials using exfoliated graphite nanoplatelets. *Solar Energy Materials & Solar Cells* 93:136–42.

Kosny, J., K. Biswas, W. Miller, and S. Kriner. 2012. Field thermal performance of naturally ventilated solar roof with PCM heat sink. *Solar Energy* 86:2504–14.

BASF. 2013. Micronal® phase change material, DS 5008 X, http://worldaccount.basf.com/wa/EU/Catalog/ACIndustry/pi/BASF/segment/new_building_materials

EIA. 2009. Residential Energy Consumption Survey (RECS). Washington, DC: U.S. Energy Information Administration. www.eia.gov/consumption/residential/data/2009/index.cfm?view=consumption

Sari, A., and A. Karaipekli. 2007. Thermal conductivity and latent heat thermal energy storage characteristics of paraffin/expanded graphite composite as phase change material. *Applied Thermal Engineering* 27(8-9):1271–77.

Sharma, A., V.V. Tyagi, C.R. Chen, and D. Buddhi. 2009. Review on thermal energy storage with phase change materials and applications. *Renewable and Sustainable Energy Reviews* 13(2):318–45.

Shrestha, S., W. Miller, T. Stovall, A. Desjarlais, K. Childs, W. Porter, M. Bhandari, and S. Coley. 2011. Modeling PCM-enhanced insulation system and benchmarking EnergyPlus against controlled field data. *Proceedings of Building Simulation 2011: 12th Conference of International Building Performance Simulation Association*, p 800–807.

Stovall, T.K., and J.J. Tomlinson. 1995. What are the potential benefits of including latent storage in common wallboard? *Journal of Solar Energy Engineering, Transactions of the ASME* 117(4):318–25.

Xin, W., Z. YinPing, X. Wei, Z. RuoLang, Z. QunLi, and D. HongFa. 2009. Review on thermal performance of phase change energy storage building envelope. *Chinese Science Bulletin* 54(6):920–28.

Zalba, B., J.M. Marin, L.F. Cabeza, and H. Mehling. 2003. Review on thermal energy storage with phase change: Materials, heat transfer analysis and applications. *Applied Thermal Engineering* 23:251–83.

Zhou, G., Y. Zhang, X. Wang, K. Lin, and W. Xiao. 2007. An assessment of mixed type PCM-gypsum and shape-stabilized PCM plates in a building for passive solar heating. *Solar Energy* 81:1351–60.